Selective adsorption and structure formation of N_2 on the nanostructured Cu-CuO stripe phase

P. Zeppenfeld,[1,*] V. Diercks,[2,†] R. David,[2] F. Picaud,[3] C. Ramseyer,[3] and C. Girardet[3]
[1]*Institut für Experimentalphysik, Johannes-Kepler-Universität Linz, A-4040 Linz, Austria*
[2]*Institut für Schichten und Grenzflächen, Forschungszentrum Jülich GmbH, D-52425 Jülich, Germany*
[3]*Laboratoire de Physique Moléculaire–UMR CNRS 6624-Faculté des Sciences, la Bouloie, Université de Franche-Comté, 25030 Besançon Cedex, France*
(Received 21 January 2002; published 15 August 2002)

The adsorption of nitrogen molecules on the nanostructured Cu(110)-Cu(110)-(2×1)O surface was studied both experimentally using He atom diffraction and thermal desorption spectroscopy as well as theoretically using a semiempirical potential approach. The substrate (referred to as the Cu-CuO stripe phase) provides a unique template for studying the adsorption, structure formation and desorption on narrow terraces (stripes) of alternating Cu(110) and Cu(110)-(2×1)O areas, whose width can be varied systematically by the amount of preadsorbed oxygen Θ_O. The adsorption of N_2 on the Cu-CuO stripe phase occurs in a selective and sequential manner according to the hierarchy of the available binding sites. The molecules are first adsorbed in a lattice gas phase on top of the CuO stripes, followed by the formation of a dense monolayer phase on the bare Cu stripes. Finally, additional molecules are adsorbed on the CuO stripes leading to a compression of the lattice gas phase. We find a substantial influence of the finite size of the stripes on the ordering of the adlayer of N_2 as compared to the adsorption on extended terraces of the homogeneous surfaces of Cu(110) ($\Theta_O=0$) and Cu(110)-(2×1)O ($\Theta_O=0.5$), respectively. On large Cu stripes ($\Theta_O<0.1$), a pinwheel structure for the N_2 monolayer is found to be stable, whereas a (4×3) compressed phase is observed on large CuO stripes ($\Theta_O>0.38$). For stripe widths below 30–50 Å ($0.1<\Theta_O<0.38$), the diffraction signatures from the orientationally ordered commensurate phases disappear in the experiment as well as in the calculated structure factors. The calculations reveal that the original structures become disordered as a result of the confinement of the N_2 layer and the strong pinning of the adlayer to the step edges separating neighboring Cu and CuO stripes. The orientational order appears to be particularly sensitive, whereas the local positional order and the preferred adsorption sites of the molecules are essentially preserved.

DOI: 10.1103/PhysRevB.66.085414 PACS number(s): 68.43.−h, 68.55.−a, 61.18.Bn

I. INTRODUCTION

The presence of steps or point defects on the surface is known to strongly influence the nucleation and growth of deposited atoms or molecules. The preferential nucleation at step edges on regularly stepped (vicinal) surfaces can, indeed, be used to grow well-ordered ''quantum wires'' or single atomic lines with a well-defined lateral arrangement and orientation enforced by the regularity of the substrate steps.[1–3] On the other hand, flat surfaces may undergo a spontaneous self-ordering during chemisorption, such as in the case of oxygen adsorption on Cu(110) (Ref. 4) or atomic nitrogen on Cu(100).[5,6] As a result a stripe [one-dimensional (1D)] or square (2D) array of regularly shaped domains separated by uncovered, bare Cu areas is formed in the submonolayer coverage regime. These patterns are quite regular and thermodynamically stable. In addition, the two alternating types of domains are chemically different and subsequent adsorption may occur *selectively* on either of the two. Such nanostructured surfaces thus provide ideal templates to study the influence of the finite domain size on the adsorption, binding, and structure formation of atoms and molecules.[7,8]

For the present case, we have studied the adsorption of molecular nitrogen on the nanostructured Cu-CuO stripe phase. As shown previously,[4,8] the adsorption of submonolayer amounts of oxygen ($\Theta_O<0.5$) and subsequent annealing results in the formation of a regular array of alternating CuO and bare Cu(110) stripes. The CuO stripes are elongated islands with monatomic height of the well known Cu(110)-(2×1) ''added'' row phase.[9] The stripes are composed of individual Cu-O rows running along the [001] direction which are separated by two Cu lattice constants along the $[1\bar{1}0]$ direction. It has been shown that the width of the CuO and Cu domains as well as the periodicity of the stripe phase can be varied systematically over in the nanometer range by simply changing the oxygen coverage Θ_O.[8] The stripe phase represents the equilibrium morphology of the surface and forms as a result of the relaxation of the surface stress. Its stability and the variation of the stripe width and periodicity with the oxygen coverage can be understood quantitatively within the framework of continuum elasticity theory.[10]

In previous investigations we have studied the adsorption of nitrogen molecules on the bare Cu(110) substrate and on the fully covered Cu(110)-(2×1)O surface, respectively. On Cu(110),[11] the N_2 molecules tend to stay within the potential troughs running along the $[1\bar{1}0]$ direction, i.e., parallel to the close packed Cu atomic rows. At the same time, the molecules seek to arrange themselves in their natural bulk hexagonal arrangement. As a result, a high-order commensurate $\begin{pmatrix}4 & 1\\ 1 & 3\end{pmatrix}$ phase is formed in which the N_2 molecules are ordered in a quasihexagonal array with a ''pinwheel type'' orientational order. As derived from the model calculations, each unit cell contains seven N_2 molecules: six of them lay flat on the surface coiling around a central ''pin'' molecule

which stands upright on the surface.[11]

In contrast, the large corrugation imposed by the Cu(110)-(2×1)O surface was shown to force the centers of mass of the N_2 molecules to stay inside the troughs between the Cu-O added rows along the [001] direction. As a consequence, N_2 molecules adopt the rectangular structure of the reconstructed surface forming a (2×1) phase in which the molecules are spaced at $2a=5.1$ Å along $[1\bar{1}0]$ and at a distance larger or equal than $2\sqrt{2}a=7.2$ Å along [001].[12,13] At these large distances, the lateral interaction between neighboring molecules is close to zero and the adlayer behaves like a lattice gas. At higher coverages the adlayer is compressed along the [001] direction and additional molecules adsorb between the potential troughs. The model calculations reveal that the (4×3) phase contains eight molecules per unit cell. Four molecules are adsorbed inside the troughs between the Cu-O rows with their axes lying flat on the surface and nearly parallel to the rows, while the remaining four molecules are adsorbed flat above the Cu-O rows and oriented approximately parallel to these rows.[12,13]

In the two limiting cases ($\Theta_O=0$ and $\Theta_O=0.5$, respectively) the N_2 surface density at monolayer completion is approximately the same ($\simeq0.07$ Å^{-2}), whereas the shape of the unit cells, the internal molecular arrangement, and the orientation of the N_2 molecules are completely different. Furthermore, the binding on the two substrates are quite different: On the CuO surface the heat of adsorption per molecule ranges from 125 ± 6 meV in the lattice gas phase to 94 ± 6 meV in the compressed (4×3) phase,[12] whereas in the $\begin{pmatrix}4 & 1\\ 1 & 3\end{pmatrix}$ phase on Cu(110) it amounts to 105 ± 6 meV.[11] The aim of this paper is to study (i) the adsorption/desorption scenario in the presence of the hierarchy of the binding energies and (ii) the influence of the lateral confinement imposed by the finite domain sizes on the structural ordering of the molecules. We use thermal He atom scattering and temperature programmed desorption (TPD) to characterize the adsorption/desorption behavior and He atom diffraction to determine the adlayer structures as a function of the domain size. Then, we compare the experimental data to minimum energy calculations using realistic potentials to describe the substrate-adsorbate and the adsorbate-adsorbate interactions.

In Sec. II, we present the experimental data on the adsorption/desorption kinetics and the adlayer structure of N_2 adsorbed on the Cu-CuO stripe phase. Section III describes the main aspects of the calculation, especially the implementation of the particular morphology of the Cu-CuO stripe phase. The numerical results are presented in Sec. IV and are compared to the experimental observations.

II. EXPERIMENTAL DATA

A. Setup and preparation

The experiments were performed in the He scattering apparatus described in Ref. 14. The Cu-CuO stripe phase was prepared by exposing the clean Cu(110) sample to oxygen at elevated surface temperature between 500 and 600 K. For exposures <10 L corresponding to oxygen coverages $\Theta_O<0.5$ a regular array of (2×1) ''added row'' reconstructed CuO stripes separated by uncovered Cu areas is obtained.[4] As an example, Fig. 1 shows an STM image and a schematic model of the stripe phase for $\Theta_O=0.25$. The width of the CuO stripes (l) and of the bare Cu areas (L) and, hence, the overall periodicity $D=l+L$ of the Cu-CuO ''stripe phase'' along the $[1\bar{1}0]$ direction are unique functions of the oxygen coverage.[8] Experimentally, the stripe phase can easily be characterized by He diffraction profiles recorded along the $[1\bar{1}0]$ direction. The long-range order of the stripe phase which acts as a nanometer scale diffraction grating leads to sharp satellite peaks around the specular reflection. The spacing between these satellite peaks yields the periodicity D. From the known oxygen coverage Θ_O the CuO stripe width is obtained as $l=2\Theta_O D$. Due to the stability of the Cu-CuO stripe phase its structure and long-range ordering is not affected by the adsorption of weakly physisorbed molecules. Indeed, after desorption of the adlayer the He diffraction pattern of the original stripe phase is fully recovered. This offers the intriguing opportunity to study the influence of the finite size of the Cu and CuO domains on the adsorption and structural properties of physisorbed molecules in comparison to the case of the homogeneous Cu(110) and Cu(110)-(2×1)O surfaces.

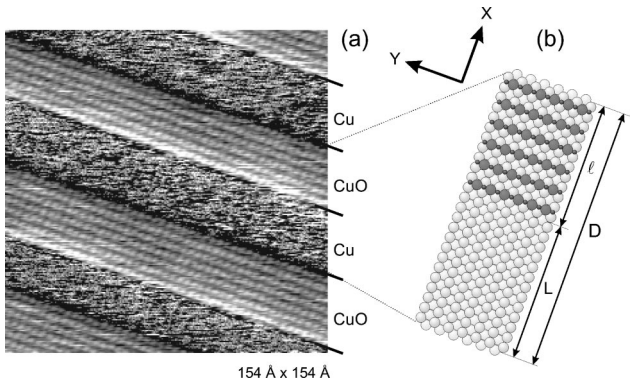

FIG. 1. STM image recorded at room temperature (a) and schematic representation (b) of the Cu-CuO stripe phase for $\Theta_O=0.25$. According to Table I the average CuO stripe width is $l=31.4$ Å (corresponding to about 6–7 Cu-O chains per stripe), and the overall periodicity is $D=62.8$ Å, which is roughly $p=25$ times the Cu lattice spacing of $a=2.55$. X and Y define the $[1\bar{1}0]$ and [001] directions, respectively.

For the present investigation the Cu and CuO domain size (stripe widths L and l, respectively) were varied systematically by using different oxygen precoverages. The selected coverages and the corresponding values for the widths l, L and for the stripe phase periodicity D are listed in Table I.

B. Adsorption of N_2 on the stripe phase

Molecular nitrogen was adsorbed from the gas phase and the formation of ordered monolayer structures was monitored using He diffraction. To study the adsorption process, the variation of the peak heights of the (0,0) specular beam and of the (1/2,0) diffraction peak were recorded as a function of exposure [Fig. 2(a)]. Due to the low He reflectivity of the highly corrugated CuO stripes, the specular intensity is

TABLE I. Periodicity D of the Cu-CuO stripe phase and width of the Cu-O stripes (l) and Cu stripes (L) as a function of the oxygen coverage Θ_O. These values were calculated from a fit to Vanderbilt's theory which gives an excellent interpolation of the experimental data (Ref. 8). Also indicated are the number of unit cells N_{CuO} and N_{Cu} of the respective N_2 superstructure which would fit on the CuO and Cu stripes along the $[1\bar{1}0]$ direction. Values in bold face indicate that the corresponding superstructure diffraction peaks were, indeed, observed experimentally.

Θ_O	D (Å)	l (Å)	L (Å)	N_{CuO}	N_{Cu}
0.12	92.0	22.1	69.8	2	**6-7**
0.19	67.6	25.7	41.9	2-3	4
0.2	66.1	26.4	39.6	2-3	4
0.22	64.0	28.1	35.8	3	3-4
0.25	62.8	31.4	31.4	3	3
0.32	69.4	44.4	25.0	4	2-3
0.34	74.4	50.6	23.8	**5**	2
0.37	86.2	63.8	22.4	**6**	2
0.42	130.4	109.6	20.9	**10-11**	2

mainly sensitive to the adsorption on the bare Cu stripes. In contrast, the (1/2,0) diffraction peak is characteristic of the oxygen induced (2×1) reconstruction and, hence, only sensitive to the adsorption on the CuO stripes. Monitoring these two intensities thus provides complementary information on *where* the adsorption takes place during N_2 exposure.

The adsorption curves depicted in Fig. 2(a) reveal a strong decrease of the (1/2,0) diffraction peak up to an exposure of about 0.8 L at which point all CuO stripes appear to be covered by nitrogen molecules. At the same time, the specular intensity also decreases but eventually reaches a local maximum at around the same exposure of 0.8 L where it is still 70% of its initial value. Only upon further exposure does

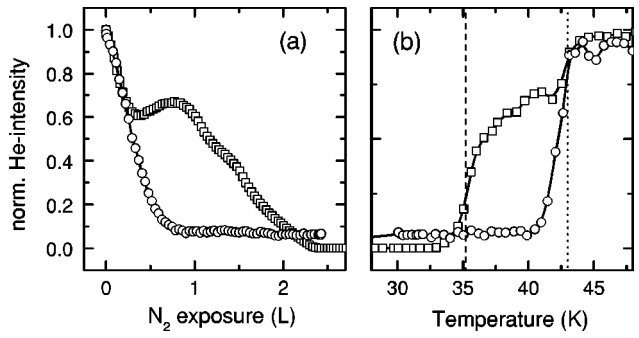

FIG. 2. Peak intensities of the (0,0) (squares) and of the (1/2,0) (circles) He diffraction peak recorded (a) during adsorption of N_2 on the Cu-CuO stripe phase at a surface temperature of 25 K and (b) during desorption of the N_2 monolayer when applying a linear heating rate of 1 K/s. The Cu-CuO stripe phase was prepared by adsorption of $\Theta_O=0.32$ of oxygen, corresponding to an area of 64% being covered by CuO stripes of $l=44.4$ Å width and stripe periodicity $D=69.4$ Å. The dotted lines in (b) indicate the temperatures at which the N_2 desorption takes place on the clean Cu(110) surface and on the completely covered Cu(110)-(2×1)O surface, respectively.

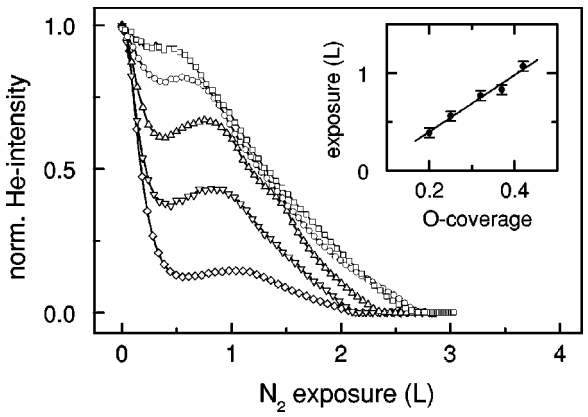

FIG. 3. N_2 adsorption curves on the Cu-CuO stripe phase with different oxygen precoverage: $\Theta_O=0.20$ (squares), $\Theta_O=0.25$ (circles), $\Theta_O=0.32$ (triangles up), $\Theta_O=0.37$ (triangles down), $\Theta_O=0.42$ (diamonds). The inset shows the position of the local maximum of these curves, i.e., the exposure required to cover the CuO stripes with N_2, as a function of the oxygen precoverage.

the specular intensity drop to zero indicating the complete coverage of the Cu stripes. The consecutive decrease of the (1/2,0) and of the specular intensity suggests an adsorption scenario in which the nitrogen molecules are first adsorbed on the CuO stripes and, when the preferential sites are all occupied, adsorption on the bare Cu stripes takes place. Note that the surface temperature in this experiment is 25 K. This temperature appears to be high enough for the physisorbed nitrogen molecules to diffuse freely across the surface and search for an energetically most favorable adsorption site. In other words, molecules impinging on a bare Cu stripe are able to reach a nearby CuO stripe where they will stick until it is completely covered.

This *selective* adsorption scenario is corroborated by the desorption experiment depicted in Fig. 2(b). After adsorption of a monolayer of N_2 on the same stripe phase ($\Theta_O=0.32$) a linear temperature ramp with a heating rate of 1 K/s was applied and the variation of the He intensities of the (0,0) and (1/2,0) diffraction peaks were recorded. It is easily recognized in Fig. 2(b) that the desorption first takes place from the bare Cu(110) areas (corresponding to the increase of the specular intensity at around 35 K). Only later, at about 42 K, the N_2 molecules desorb from the CuO stripes, leading to the sudden increase of the intensity of the half-order peak and the complete recovery of the specular peak. The desorption sequence is just reversed to that of the adsorption in Fig. 2(a). The higher desorption temperature is clearly related to the larger binding energy of the N_2 molecules on Cu(110)-(2×1)O as compared to the bare Cu(110) surface.[11,12] For comparison the desorption temperatures (steepest intensity rise) for the bare ($\Theta_O=0$) and for the completely oxygen covered Cu(110) surface ($\Theta_O=0.5$) are indicated in Fig. 2(b) by the dashed and the dotted line, respectively.

For a more quantitative analysis of the adsorption process, Fig. 3 shows the N_2 adsorption curves recorded at 25 K on Cu-CuO stripe phases with different amounts of preadsorbed oxygen Θ_O and, hence, different surface fractions $2\Theta_O$ cov-

ered by CuO stripes. As in Fig. 2(a), the maximum of the specular intensity occurs when the selective adsorption of N_2 on the CuO stripes is complete. In the inset of Fig. 3 the corresponding exposures are plotted as a function of Θ_O. The straight, linear relationship between these exposures and the CuO surface fraction confirms the initial, selective adsorption of N_2 on the CuO stripes. The amount required to cover a *fully* oxygen covered Cu(110)-(2×1)O surface ($\Theta_O=0.5$) can be extrapolated from the data to be 1.3 L. This value is much smaller than the amount of 2.8 L required for monolayer completion and saturation of the (4×3) phase.[12] On the other hand, 1.3 L corresponds exactly to the amount for completion of the (2×1) lattice gas phase. We may, therefore, conclude that the first step in the adsorption on the stripe phase consists in the formation of an uncompressed (lattice gas) phase on the CuO stripes. Once this phase is saturated, adsorption proceeds on the bare Cu stripes. In fact, as will be shown later, only in a third step (after the Cu stripes have been covered with nitrogen), molecules are again adsorbed on the CuO stripes leading to the final compression of the adlayer into a compressed phase similar to the (4×3) phase on the Cu(110)-(2×1) surface. Indeed, this three-step selective adsorption scenario is quite consistent with the hierarchy of the adsorption energies of 125, 105, and 94 meV for the (2×1) gas phase on CuO, the $\begin{pmatrix}4 & 1\\ 1 & 3\end{pmatrix}$ phase on Cu, and the (4×3) phase on CuO, respectively.[11,12]

C. Structure of N_2 on the stripe phase

An intriguing question is to what extend the positional and orientational ordering of the N_2 molecules is affected by the finite size of the Cu and CuO stripes. As already mentioned, the structure, intermolecular arrangement and the orientation of the molecules is known to be quite different on the Cu(110) and the Cu(110)-(2×1) surface, respectively. The unit cells of the $\begin{pmatrix}4 & 1\\ 1 & 3\end{pmatrix}$ and (4×3) monolayer phases on Cu and CuO, respectively, are rather large. Depending on the oxygen coverage Θ_O the stripes may accommodate a few unit cells of the original structures, only (see Table I). In addition, the step edges along the [001] directions separating neighboring Cu and CuO stripes could have a marked influence on the ordering of the adsorbed molecules.

He diffraction was used to investigate the ordering and structure formation during adsorption of N_2 on the stripe phase. In particular, the appearance of the most intense diffraction peaks of the $\begin{pmatrix}4 & 1\\ 1 & 3\end{pmatrix}$ phase observed on the bare Cu(110) surface[11] and of the $(0,m/3)$ diffraction spots characteristic of the (4×3) monolayer structure of N_2 on the completely oxygen covered Cu(110)-(2×1)O surface were monitored as a function of coverage and for different stripe widths.[15] The results are summarized in Fig. 4. The peak intensities of the two reference structures were normalized to the intensities measured on the homogeneous Cu and CuO surfaces, respectively. No significant diffraction intensities from either the $\begin{pmatrix}4 & 1\\ 1 & 3\end{pmatrix}$ nor the (4×3) phase can be observed for intermediate oxygen coverages $0.2\leqslant\Theta_O\leqslant0.3$, i.e., for stripe phases where the width of the Cu and CuO stripes are smaller than about 50 Å (see Table I). On the other hand, for

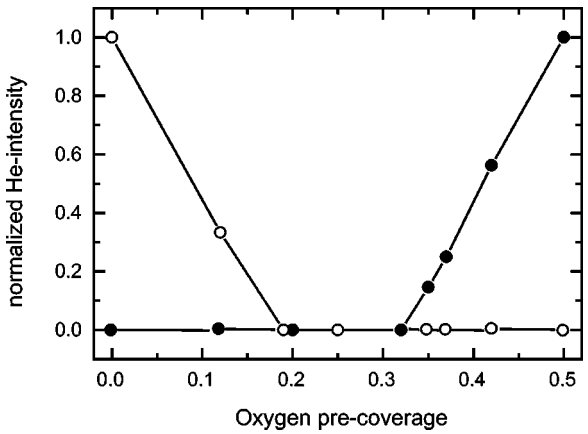

FIG. 4. Peak intensities (recorded at 25 K) of the most intense N_2 superstructure diffraction spots of the $\begin{pmatrix}4 & 1\\ 1 & 3\end{pmatrix}$ phase (open circles) and the (4×3) phase (filled circles) recorded from the N_2 monolayer adsorbed on the Cu-CuO stripe phase for different oxygen precoverages. The intensities are normalized to the values obtained for the homogeneous Cu and CuO surfaces, $\Theta_O=0$ and $\Theta_O=0.5$, respectively.

lower (higher) oxygen coverages where the Cu (CuO) stripe widths exceed 50 Å the same diffraction patterns as on the homogeneous surfaces are obtained.

As indicated in Table I the ''critical'' stripe width above which the $\begin{pmatrix}4 & 1\\ 1 & 3\end{pmatrix}$ and (4×3) structures can be observed is such that at least 5–6 N_2 unit cells of the respective phase can be placed on the Cu or CuO stripes along the short $[1\bar{1}0]$ direction. Since the diffraction intensities are expected to decrease significantly with decreasing number of coherently scattering N_2 unit cells, it cannot be excluded on the basis of these diffraction experiments whether the disappearance of the diffraction signal is simply related to the eventual decrease of the peak intensity below the detection limit rather than to the actual disappearance of the superstructure itself. To decide between ''coherence'' and ''finite size'' effects, model calculations were performed which are presented in Sec. III.

Figure 5 shows the diffraction profiles for three characteristic situations: (i) large Cu stripes ($\Theta_O=0.12$), (ii) equally sized, small Cu and CuO stripes ($\Theta_O=0.22$), and (iii) large CuO stripes ($\Theta_O=0.42$). As already mentioned, the $\begin{pmatrix}4 & 1\\ 1 & 3\end{pmatrix}$ phase is observed in case (i) and the (4×3) phase in case (iii). Note, however, that the intensity of the diffraction peaks is much smaller than for the adsorption on extended terraces on the Cu(110) and the Cu(110)-(2×1)O surface, respectively.[11,12]

Although no N_2 related superstructure peaks are obtained in case (ii) above, an interesting diffraction profile [Fig. 5(c)] was obtained after adsorption of 0.8 L of N_2 in this case. The profile reveals the known satellite peaks[4] around the integer diffraction peaks (0,0) and (1,0) with a spacing of $\Delta Q=2\pi/D=0.1$ Å^{-1} expected for a stripe phase periodicity $D=64$ Å. In addition, however, another series of satellites with *twice* this spacing has emerged around the (1/2,0) peak at $Q=1.23$ Å^{-1}. Consequently, these satellite peaks point to a change in the surface morphology as seen by the He atoms

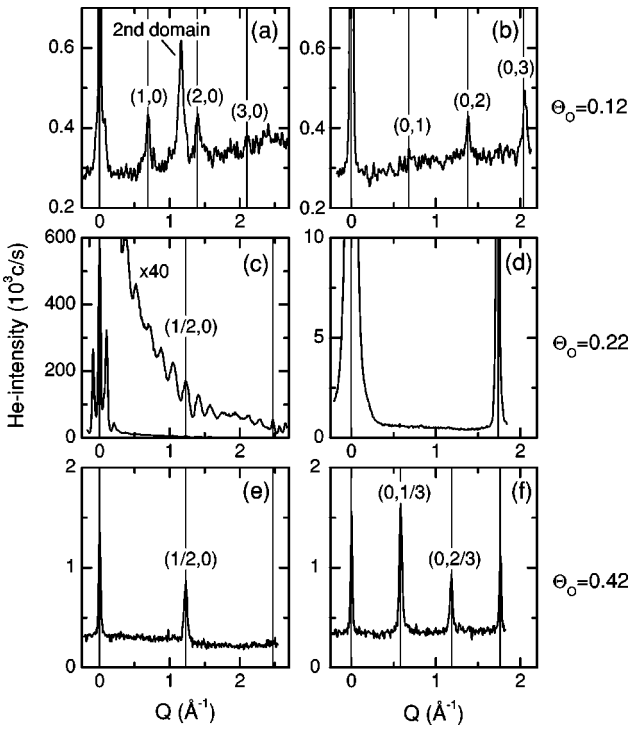

FIG. 5. He diffraction profiles recorded after adsorption of N_2 on the Cu-CuO stripe phase with different oxygen precoverage $\Theta_O=0.12$, 0.22, and 0.42 (from top to bottom). (a) and (b) were recorded after adsorption of a complete monolayer (3.2 L) of N_2 at 25 K along the $\binom{4}{1}\ \binom{1}{3}$ symmetry axes rotated by 13.3° (a) and 70.5° (b) against the $[1\bar{1}0]$ direction. (c) and (d) were recorded along the $[1\bar{1}0]$ and [001] directions, respectively, after adsorption of 0.8 L of N_2 at 25 K which corresponds to an exposure slightly beyond the intermediate maximum of the adsorption curve (see Fig. 3). (e) and (f) were recorded after monolayer saturation (2.4 L of N_2 at 25 K) along the $[1\bar{1}0]$ and [001] directions, respectively.

which is induced by the adsorption of N_2. The new periodicity corresponds to a spacing of $D/2$. Since an actual modification of the original stripe phase structure by the weakly physisorbed N_2 molecules can be excluded, we interpret this change as a modification of the electronic corrugation upon N_2 adsorption which is actually sensed by the He atoms.

Two observations have helped to understand this peculiar phenomenon in more detail. (i) The new satellites and, hence, a period of $D/2$ is only observed if the oxygen precoverage is in the range $0.2<\Theta_O<0.3$, i.e., if the Cu and CuO stripes have about equal widths. (ii) The satellites have the highest intensity if the N_2 exposure is just about (but slightly above) the amount required to completely cover the CuO stripes. In fact, the appearance of the new satellite peaks can also be identified in the adsorption and desorption curves (Fig. 6) as a small intermittent rise of the (1/2,0) peak intensity. The offset by about 0.2 L with respect to the local maximum of the specular peak indicates that also a few sites on the bare Cu stripes have already been occupied. The offset is consistent with the amount needed for the complete decoration of the lower step edges between the Cu and the CuO stripes. This strongly suggests that the step edges play an

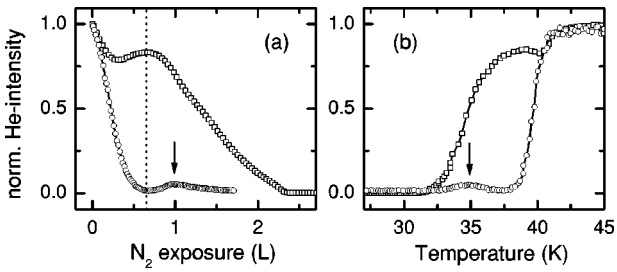

FIG. 6. Intensities of the (0,0) (squares) and of the (1/2,0) (circles) He diffraction peak recorded (a) during adsorption of N_2 on the Cu-CuO stripe phase at a surface temperature of 25 K and (b) during desorption of the N_2 monolayer when applying a linear heating rate of 1 K/s. The oxygen precoverage was $\Theta_O=0.25$, where the widths of the Cu and CuO stripes are exactly equal. Similar curves with a characteristic intermittent intensity rise (arrows) were obtained for oxygen precoverages in the range $0.2<\Theta_O<0.3$.

important role in producing the diffraction signature. Indeed, for $\Theta_O\sim 0.25$ the spacing between these steps is most regular and equals $D/2$.

As a result, we propose the following explanation: The adsorption of N_2 on the CuO stripes appears to smoothen the electronic corrugation related to the oxygen induced (2×1) reconstruction such that the main contrast in the surface morphology seen by the He atoms is dominated by the contribution of the step edges—at least within the relevant Q range around $Q=1.23$ Å^{-1}.

Monitoring the peak intensity of the diffraction peaks characteristic of the compressed (4×3) phase on the CuO stripes as a function of coverage, provides the final proof of the selective adsorption scenario. As an example, Fig. 7 shows the He intensity of the specular (0,0), the (1/2,0), and the (0,1/3) peaks during adsorption of N_2 on the Cu-CuO stripe phase with $\Theta_O=0.42$. As discussed in Sec. II B the specular and half order intensities reveal the completion of the (2×1) lattice gas phase at around 1.1 L and the subsequent adsorption on the bare Cu stripes. Finally, at around

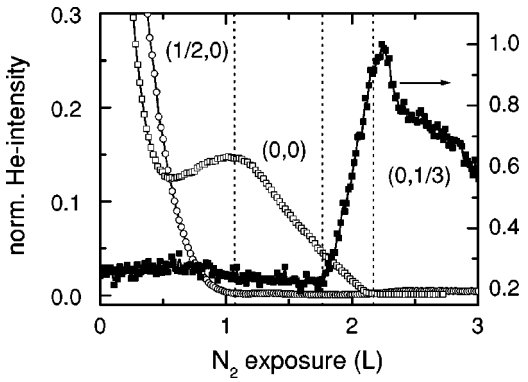

FIG. 7. He intensity of the (0,0) (open squares), the (1/2,0) (open circles), and the (0,1/3) (filled squares) diffraction peaks during adsorption of N_2 at 25 K on the Cu-CuO stripe phase with $\Theta_O=0.42$. Note the sudden rise of the (0,1/3) intensity characteristic of the (4×3) phase, marking the final compression of the N_2 monolayer.

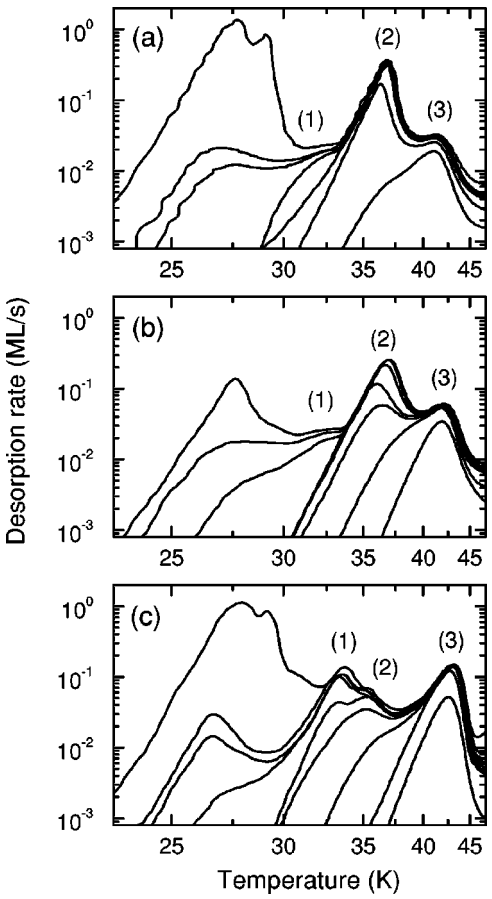

FIG. 8. Temperature programmed desorption (TPD) traces for different N_2 exposures at 20 K on the Cu-CuO stripe phase with (a) $\Theta_O=0.13$, exposures between 0.24 L and 6 L, (b) $\Theta_O=0.23$, exposures between 0.44 L and 8 L, and (c) $\Theta_O=0.42$, exposures between 0.41 L and 8 L.

1.8 L, a sudden rise of the (0,1/3) peak intensity is observed, indicating the formation of a dense (4×3) phase on the CuO stripe phase. As already mentioned, this three-step selective adsorption scenario reflects the decrease of the adsorption energies from 125 to 105 and 94 meV associated with the (2×1) gas phase on CuO, the $\left(\begin{smallmatrix}4 & 1\\ 1 & 3\end{smallmatrix}\right)$ phase on Cu, and the (4×3) phase on CuO, respectively.[11,12]

D. Temperature programmed desorption

We have explained the selective adsorption of N_2 on the Cu-CuO stripe phase in terms of the hierarchy of the adsorption energies within the different phases on the CuO and Cu stripes. Indeed, the He intensities recorded during thermal desorption [see, e.g., Fig. 2(b)] reveal a pronounced difference in the respective desorption temperatures. Rather than measuring the He diffraction signal from the remaining adlayer the desorbing molecules can be detected directly in a mass spectrometer. Such temperature programmed desorption (TPD) traces are shown in Fig. 8 for various initial N_2 coverages on three different stripe phases [$\Theta_O=0.13$ (a), 0.23 (b), and 0.42 (c)]. In the monolayer range (desorption temperatures above 30 K) three distinct desorption peaks can be distinguished. They can be associated with the desorption from the (4×3) phase on CuO (1), the $\left(\begin{smallmatrix}4 & 1\\ 1 & 3\end{smallmatrix}\right)$ phase on Cu (2) and the (2×1) gas phase on CuO (3). The desorption occurs in the reverse order as the adsorption, with the high-temperature peak (3) corresponding to the most strongly bound N_2 species on the CuO stripes. Note that with increasing oxygen precoverage the desorption peaks (1) and (3) become more pronounced whereas the N_2/Cu peak (2) decreases. This is, indeed, expected if the peaks (1) and (3) are both related to N_2 molecules adsorbed on the CuO stripes—just in different phases.

III. CALCULATIONS

A. Geometry of the Cu-CuO stripe phase

A model of the Cu-CuO stripe phase is shown in Fig. 1(b). For the bare Cu(110) surface, we consider a discrete, rigid substrate with lattice parameter $a=2.55$ Å. The unit cell is rectangular with primitive vectors of length a and $\sqrt{2}a$ and the interplanar distance is equal to $a/2$. The Cu(110)-(2×1)O substrate is modeled by adding a well ordered (2×1) CuO slab above the previous Cu(110) substrate according to the added row model of the oxygen induced reconstruction of the Cu(110) surface.[9] Whereas the lateral symmetry and the Cu-O arrangement is well established, the relative heights of the oxygen and copper atoms with respect to the Cu(110) substrate have been a subject of controversy. Here, we adopt the parameter values given in Ref. 13, obtained by fitting the adsorption properties of Xe and N_2 on Cu(110)-(2×1)O. The so determined height of the oxygen atoms with respect to the Cu added rows $d_O=-0.21\pm0.10$ Å and the height of the topmost Cu interlayer distance $d_{12}=1.60\pm0.05$ Å are close to the average of the various experimental values of $d_O=-0.09\pm0.14$ Å and $d_{12}=1.54\pm0.06$ Å, respectively.[13]

The Cu-CuO stripe phase is described by a regular sequence of $n\leqslant p/2$ CuO added rows in a (2×1) arrangement located on top of $p\leqslant p_m$ Cu rows [Fig. 1(b)]. The maximum value p_m has been chosen to be large enough to exclude finite size errors and sufficiently small to reduce computation time. The corresponding oxygen coverage Θ_O, stripe widths, and periodicity are related to the values n and p via $\Theta_O=n/p$, $D=pa$, $l=2na$, and $L=(p-2n)a$. The two limiting cases, the bare Cu(110) surface and the fully oxygen covered Cu(110)-(2×1)O surface are obtained for $n=0$ and $n=p/2$, respectively.

B. Interaction potentials

The interaction potential $V(\mathbf{R},\mathbf{\Omega})$ between the N_2 molecules and the Cu and CuO domains is the sum of an intralayer contribution V_{AA} and an adsorbate-substrate contribution V_{AS}. It depends on the position $\mathbf{R}$ of the centers of mass of the N_2 molecules and on the orientation $\mathbf{\Omega}$ of their molecular axes. The dominant interaction terms in V_{AA} are the quantum dispersion-repulsion contribution supplemented by the direct electrostatic quadrupolar interactions. Screening effects due to the substrate mediated contributions on both quantum and electrostatic potential have been shown to re-

main negligible and unable to change the structural properties of the N_2 layer.[12] The quantum interactions are described by pairwise Lennard-Jones (LJ) potentials, whereas a distributed charge description over molecular sites is used for the electrostatic term. A three point charge distribution model was shown to be adequate for N_2, with two charges equal to -0.405 a.u. located at the center of each nitrogen atom and one charge equal to $+0.810$ a.u. at the N_2 center of mass.[11] The adsorbate-substrate potential V_{AS} contains dispersion-repulsion terms similarly described by Lennard-Jones form and electrostatic interactions when necessary (i.e., on the CuO domains). The close expression of the interaction potential and the set of parameters used are given in Refs. 11–13. The ionic charges q for the Cu and O species within the Cu-O added rows were taken to be equal to $+0.8e$ and $-0.8e$, respectively,[13] whereas the Cu atoms in deeper layers do not bear any charge.

IV. NUMERICAL RESULTS AND DISCUSSION

A. Low coverage regime

In a first step, we determine the equilibrium adsorption energy of a single N_2 molecule on several characteristic sites of the Cu-CuO stripe phase for different configurations (p,n). We use a conjugate gradient minimization procedure to calculate the potential minima with respect to the binding distance and to the molecular orientation $\mathbf{\Omega}=(\theta,\varphi)$ of the N_2 molecule. For stripe phase configurations (p,n) containing more than two CuO rows $(n\geqslant 2)$, we find that the most stable site is located on the CuO stripe at a bridge site between two oxygen atoms belonging to adjacent CuO added rows. At this site, the binding energy is 121 meV, the molecular axis lies flat on the surface $(\theta=90°)$ and is parallel to the CuO chains $(\varphi=90°)$. On the Cu stripes, the N_2 molecule lies flat inside the Cu troughs with its axis along the $[1\bar{1}0]$ direction of these troughs and the binding energy is clearly weaker (83 meV).

The corrugation experienced by a single N_2 molecule moving along the $[1\bar{1}0]$ direction (Fig. 9) is the same as for the two extended surfaces[11,12] except at the boundary between the Cu and CuO stripes. Along this direction, i.e., perpendicular to the CuO rows, the corrugation is rather high on the CuO stripes (55.0 meV) in contrast to only 4 meV on the bare Cu stripes. The influence of the step edge forming the boundary between the two stripes is short ranged, extending over two lattice constants, only. On the upper step edge (CuO stripe), the N_2 molecule experiences a barrier of 60 meV, i.e., an additional step edge barrier of 5 meV, to descend onto the bare Cu stripe. At the lower step edge the molecule is trapped in a well with a depth of 104 meV. The site at the lower step is more stable than a Cu terrace site far away from the step due to the increase of the coordination number, but smaller than on the CuO stripe. The fact that the binding energy at the step edge is intermediate between the binding energies on the bare Cu and the CuO terraces results from the competition between two contributions: (i) an enhanced attraction from the dispersion contribution to V_{AS} due to the larger coordination number vs (ii) a repulsive contribution originating from the electrostatic interactions between the N_2 molecule and the CuO added rows. The binding energy at this site is only slightly more attractive than another configuration (100 meV) where the N_2 molecule still lies flat on the surface but with its molecular axis oriented *along* rather than perpendicular to the step edge. As shown below, the occurrence of two nearly equivalent sites with perpendicular orientations of the molecular axis will be of great importance for the structural ordering of the N_2 adlayer.

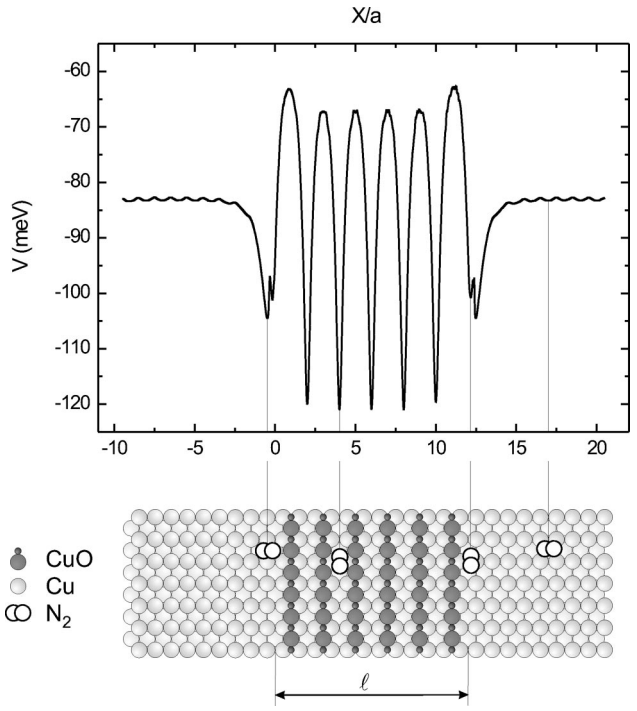

FIG. 9. Potential energy profile V_{AS} experienced by a N_2 molecule moving along the $[1\bar{1}0]$ direction on a stripe phase with $n=6$ CuO rows and a periodicity of $p=30$ Cu rows ($\Theta_O=0.2$, $l=30.6$ Å, $D=76.5$ Å). The length scale is given in units of the Cu lattice parameter $a=2.55$ Å. Also shown are the two possible configurations of an N_2 molecule at the step edge with slightly different binding energies.

B. Monolayer coverage regime

The above results on the adsorption of a single N_2 molecule are used to choose the best strategy to determine the adsorption properties of the N_2 monolayer on the stripe phase. In fact, it is rather difficult to find the N_2 molecular density for such a complicated surface geometry. Here we consider that the monolayer coverage is reached when additional molecules prefer to adsorb above the first N_2 layer instead of being directly bound to Cu or a CuO added row. As a result, the area per molecule in the first layer ranges between 14 and 16 $Å^2$ which is of the same order as the values typically obtained for N_2 adsorbed on other substrates such as Pt, Ag, or graphite.[16–20] Note that the so determined monolayer coverages are based on interaction potentials, only, and the values could slightly change if thermodynamic arguments were considered.

The equilibrium geometry of N adsorbed molecules is obtained by minimizing the total potential V with respect to the $5N$ variables which characterize the N molecules adsorbed on the Cu-CuO stripe phase. Each molecule has three translational (X,Y,Z) and two rotational (θ,φ) degrees of freedom attached respectively to its center of mass $\mathbf{R}$ and to its orientation $\mathbf{\Omega}$. For sufficiently large N, the conjugated gradient procedure fails and statistical techniques are more convenient. Simulated annealing (SA) has been shown to be one of the most efficient methods for optimization in such systems.[21] It prevents the system to be trapped in local minima and ensures to obtain a reliable equilibrium configuration. For details on the SA method and its algorithm, the reader is referred to Ref. 19. We have defined periodic boundary conditions along the CuO stripe direction in order to prevent finite size effects which could introduce frustration in this direction. A too large density of N_2 molecules in the defined box could also lead to artificial structures. These precautions were taken for all (p,n) surfaces. Typically, a box of (65 Å$\times$36 Å) containing about 200 molecules was a good compromise for obtaining a reliable equilibrium configuration at a reasonable CPU time. The starting configurations for the N_2 molecules were the $\binom{4\ \ 1}{1\ \ 3}$ pinwheel phase on the Cu domain and the (4×3) phase on the CuO stripes. Additional molecules were introduced near the Cu/CuO step edges to obtain the optimum N_2 density. In order to characterize the positional ordering of the N_2 molecules on the CuO and on the bare Cu stripes we have calculated the two structure factors

$$F_j(\mathbf{k}) = \frac{1}{N_j}\left|\sum_{n=1}^{N_j} \exp(i\mathbf{k}\cdot\mathbf{R}_j)\right|^2$$

for the N_1 molecules adsorbed on the CuO stripes $(j=1)$ and for the N_2 molecules adsorbed on the bare Cu stripes $(j=2)$. The wave vectors $\mathbf{k}$ were chosen to lie within the Cu(110) 2D reciprocal unit cell. Finally, the corresponding polar and azimuthal orientations of the N_2 molecules were determined by plotting the angular distributions $g(\theta_j)$ and $g(\varphi_j)$, respectively.

1. N_2 *on large CuO stripes* ($\Theta_O \geq 0.38$)

In Fig. 10, we show a snapshot [Fig. 10(a)] and the corresponding structure factor [Fig. 10(b)] obtained for N_2 adsorbed on large CuO stripes. For $\Theta_O = 0.38$, i.e., $n=10$ and $p=26$, the structure factor of the complete monolayer clearly exhibits spots that are characteristic of a (4×3) phase. In this case the N_2 adlayer adopts the same structure as on the extended terraces of the Cu(110)-(2×1)O surfaces.[12,13] In fact, this phase has a (2×3) periodicity if only the N_2 centers of mass are considered but slight changes in the N_2 orientations increase the unit cell by a factor of 2 along the $[1\bar{1}0]$ direction. This feature has already been discussed in Refs. 12,13. A close examination of the snapshot in Fig. 10(a) further reveals that the (4×3) unit cell contains eight molecules, half of them located above the Cu-O added rows and the other half within the troughs between these rows. The position of the molecular centers of mass is almost the same as for an infinite CuO terrace. The angular distributions show that the molecules lie flat on the surface ($\theta=90°$) with their axes oriented parallel to the Cu-O rows, along the [001] direction ($\varphi=90°$). On the narrow adjacent Cu stripe, no long-range N_2 ordering occurs whereas the molecules still remain inside the troughs formed by the close-packed Cu rows. Yet, the preferred lattice sites and the short-range positional ordering on the two stripes is rather insensitive to the confinement and the presence of the step edge. Only the pinwheel orientational ordering on the bare Cu area appears to be suppressed almost completely. As expected from the potential corrugation (Fig. 9), the influence of the step edges is of short range and only the positions and the azimuthal orientations of the molecules closest to the step edge are significantly altered. The adsorption energies on the large CuO terraces are the same as those obtained on the extended CuO substrate, namely, 122 meV for the lattice gas structure and about 100 meV for the additional N_2 molecules adsorbed on the CuO stripes for the compressed (4×3) phase.[12] As a result, the *average* adsorption energy in the compressed (4×3) phase amounts to 102.5 meV per molecule.

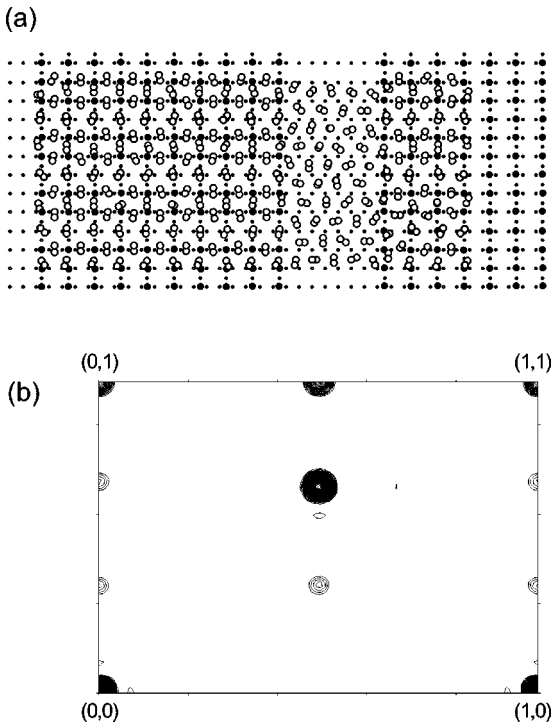

FIG. 10. (a) Snapshot of the N_2 monolayer adsorbed on the $(p,n)=(26,10)$ Cu-CuO stripe phase. Black circles correspond to oxygen atoms, small dots to Cu atoms, and pairs of large white circles represent N_2 molecules (total number of molecules: $N=226$). (b) Structure factor obtained by considering only the molecules adsorbed on the CuO stripe. The spots are characteristic of the (4×3) phase.

2. N_2 *on large Cu stripes* ($\Theta_O \leq 0.1$)

The other limiting case where the N_2 molecules are adsorbed on large Cu areas and correspondingly narrow CuO stripes ($p=28$, $n=2$, $\Theta_O=0.07$) is represented in Fig. 11.

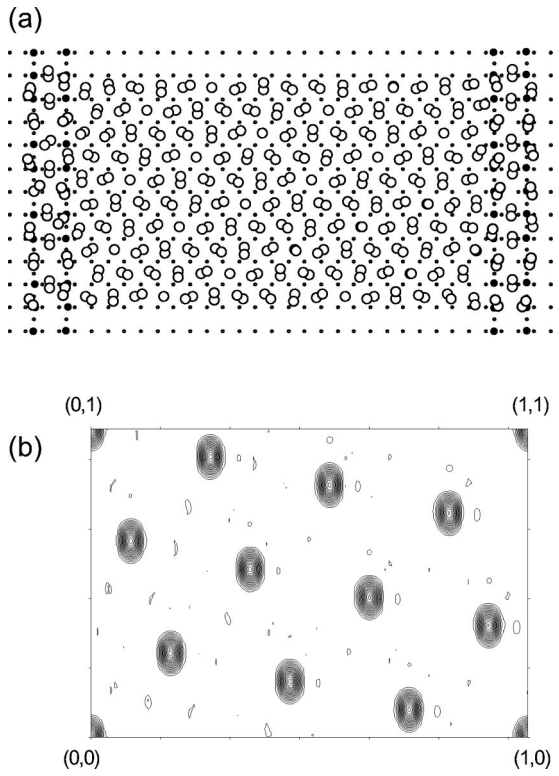

FIG. 11. (a) Snapshot of the N_2 monolayer adsorbed on the $(p,n)=(28,2)$ Cu-CuO stripe phase (total number of molecules: $N=221$). (b) Structure factor obtained by considering only the molecules adsorbed on the Cu stripe. The spots are characteristic of the $\begin{pmatrix} 4 & 1 \\ 1 & 3 \end{pmatrix}$ phase.

Figure 11(a) shows that no long-range order exists on the narrow CuO stripes. The lateral arrangement is nevertheless consistent with the preferred lattice sites obtained in the previous section for a single N_2 molecule in the vicinity of the step edge. The orientations of the molecules are again much more sensitive. Indeed, the distributions of the polar and azimuthal angles are quite broad: $\theta=90°\pm20°$ and $\varphi=80°\pm40°$, respectively. Above the wide Cu stripe, the snapshot in Fig. 11(a) and the structure factor [Fig. 11(b)] associated with this phase show that the pinwheel arrangement obtained on the extended Cu(110) terraces[11] is clearly present on a Cu stripe of about 60 Å wide. Also the same well ordered $\begin{pmatrix} 4 & 1 \\ 1 & 3 \end{pmatrix}$ superstructure as in the case of N_2 adsorbed on the bare Cu(110) surface[11] is obtained. The unit cell contains six molecules lying flat on the surface which coil around one upright molecule. Since the orientation of the unit cell is oblique with respect to the [001] direction of the step edge, we conclude that its influence is not strong enough to modify the overall translational symmetry of the adlayer. In fact, the influence of the step edge extends over two to three Cu lattice sites, only. In the vicinity of the step, the molecular centers of mass are shifted from their position in the ideal pinwheel lattice and, in particular, the molecular orientations are appreciably perturbed. Indeed, the proportion of pin molecules is reduced from 1/7 in the ideal case to about 0.12 since the supposed pin molecules are likely to tilt down to $\theta=90°$ in the vicinity of the step due to the presence of the two step wells with flat molecular orientation (see Fig. 9 and Sec. IV A). On the other hand, the azimuthal distribution $g(\varphi)$ is not strongly affected by the step edge since the three privileged directions ($\varphi=30°$,90°, and 120°) remain nearly unchanged and the equipartition of the molecules in the three directions is preserved. The average binding energy per N_2 molecule on the large Cu stripes is found to be 114 meV [the same as on the extended Cu(110) surface]. On the narrow CuO stripe the average energy in the (4×3) phase becomes 106 meV, a value slightly larger than on the extended terraces of the Cu(110)-(2×1)O surface (102.5 meV). The small increase is due to the lateral interaction with the molecules adsorbed on the neighboring Cu stripe at the bottom of the step edge.

3. N_2 *adsorption in the intermediate case* ($0.1<\Theta_O<0.38$)

The situation where the CuO and Cu stripes have comparable width is shown in Fig. 12 for $p=26$, $n=6$, and thus $\Theta_O=0.23$. On the CuO stripe, the centers of mass of the molecules are slightly displaced along the [001] direction with respect to the ideal positions in the (4×3) phase [Fig. 12(a)]. In fact, some spots in the (4×3) reciprocal lattice [Fig. 12(b)], namely, the (0,1/3) and the (0,2/3) spots, are strongly attenuated or even disappear completely. On the Cu stripe the snapshot shows a reduced translational order and the absence of a pinwheel type orientational order. This is corroborated by the lack of significantly intense peaks in the structure factor [Fig. 12(c)]. Nevertheless, the centers of mass, remain inside the potential troughs along the $[1\bar{1}0]$ direction, and tend to respect their natural hexagonal arrangement. On the CuO stripes, the average N_2 adsorption energy is equal to 120 meV in the lattice gas phase and 102.5 meV in the (4×3) compressed phase. On the Cu stripes, the binding energy is equal to 109 meV. It should be noted that the pinwheel structure becomes a metastable phase with a binding energy per molecule slightly lower (104 meV per molecule) as compared to the orientationally disordered phase (109 meV).

V. COMPARISON WITH EXPERIMENTAL DATA AND DISCUSSION

From the analysis of the adsorption on the Cu-CuO stripe phase, we find that the binding energies per molecule are only slightly affected, except for the molecules adsorbed at the lower step edges on the Cu stripes (Fig. 9). For instance, the average binding energy per molecule on a Cu stripe of width $L=14a=36$ Å (Sec. IV B 3) amounts to 109 meV as compared to 114 meV on the extended, bare Cu substrate. Likewise, the binding energy per molecule in the distorted (4×3) phase on a small CuO stripe (106 meV, see Sec. IV B 2) is similar to the one calculated for the compressed N_2 monolayer on the Cu(110)-(2×1)O surface (102.5 meV). In the low coverage regime the (2×1) lattice gas is stable with a binding energy per molecule of about 120–125 meV on large CuO terraces, and the binding strength is reduced by a few meV in the immediate vicinity of the upper step edge, only (Fig. 9).

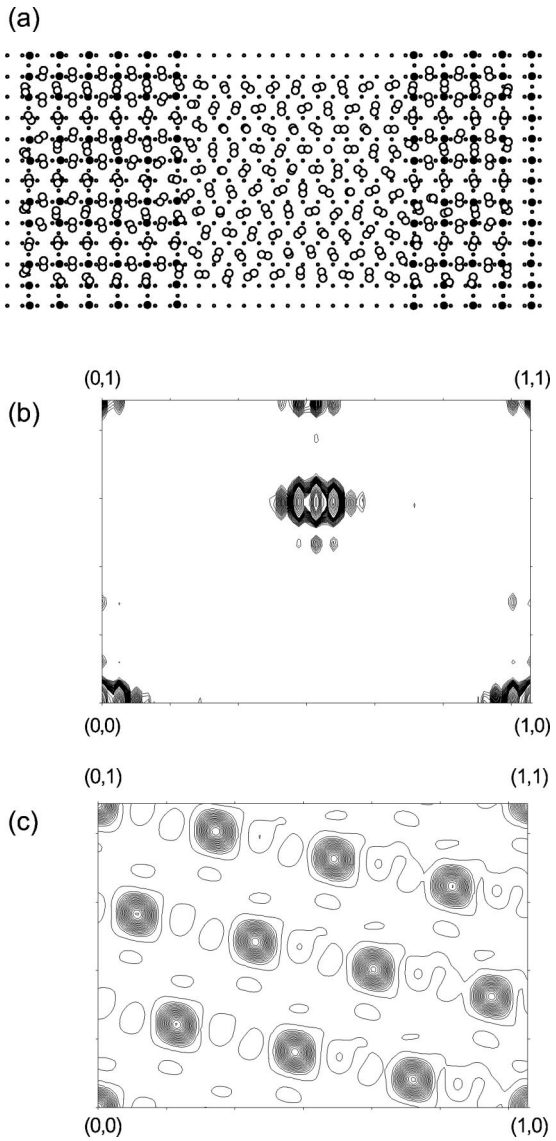

FIG. 12. (a) Snapshot of the N_2 monolayer adsorbed on the $(p,n)=(26,6)$ Cu-CuO stripe phase (total number of molecules: $N=201$). (b) and (c) structure factors calculated by considering the molecules adsorbed on the CuO and the Cu stripes, respectively.

This nicely supports the experimental results and the adsorption scenario inferred from the adsorption, diffraction, and thermal desorption measurements. Indeed, the hierarchy of the binding energies is confirmed in the calculation and it appears that the Cu-CuO stripe phase can be viewed as a template on which the adsorption and desorption proceeds in a well defined *selective* way: (i) the N_2 molecules will adsorb on the CuO stripes which provide the strongest binding sites (120–125 meV) until a dense lattice gas is formed. (ii) Prior to the compression of this phase, however, it is energetically favorable to cover the Cu stripes with a N_2 monolayer (109–114 meV). (iii) Finally, molecules are again adsorbed on the CuO stripes leading to the formation of a slightly disordered (4×3) phase (102.5–106 meV). Hence, the corresponding energy bias associated with the transitions (i),(ii) and (ii),(iii) can be calculated to be of the order of $\Delta E\simeq 11$ and 8 meV, respectively. These values should be compared to those estimated from the measured binding energies on the *extended* substrates,[12] namely, $\Delta E=125-105=20$ meV and $105-94=11$ meV, respectively.

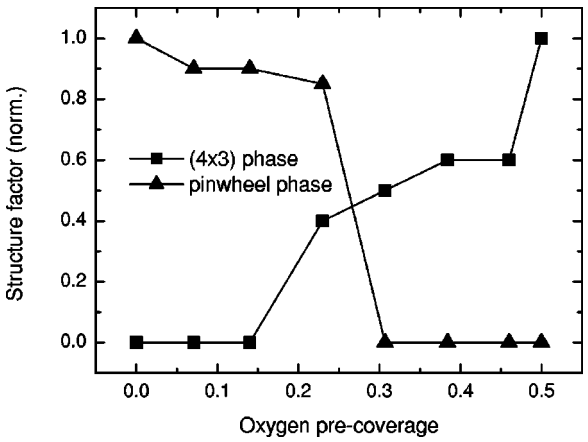

FIG. 13. Variation of the calculated peak intensity of the (0,1/3) and $(3,0)_{N_2}$ peaks connected, respectively, to the (4×3) structure on CuO and to the $\begin{pmatrix}4 & 1\\ 1 & 3\end{pmatrix}$ pinwheel phase on Cu as a function of the oxygen coverage Θ_O.

Regarding the relative stability of the (4×3) and pinwheel phases as a function of the Cu/CuO stripe widths, we have plotted in Fig. 13 the maximum values of the (0,1/3) and the $(3,0)_{N_2}$ superstructure spots (Fig. 5), characteristic of these two phases. The result should be compared to the experimental data shown in Fig. 4. At low oxygen coverage ($\Theta_O<0.2$), corresponding to a CuO stripe width $l\leqslant 25$ Å, the (0,1/3) spot can no longer be observed. The reverse situation is obtained for the $(3,0)_{N_2}$ spot, which disappears at around $\Theta_O=0.25$, i.e., if the Cu stripes become narrower than about 30 Å.

This behavior is in qualitative agreement with the diffraction data summarized in Fig. 4, although the measured intensities appear to be more affected by the finite domain size than predicted by theory. In particular, the critical stripe width below which either of the two phases can no longer be detected is about 50 Å, i.e., almost twice as large as in the calculation. Of course, a quantitative comparison of the structure factor (calculated within the simple kinematic approximation) and the measured He peak intensity is not possible. In fact, the dynamic nature of the scattering process should be taken into account as well as the presence of steps leading to strong diffuse scattering. Also, the presence of surface imperfections, such as kinks along the step edges could significantly deteriorate the long-range ordering.

From the snapshots in Figs. 10–12 we may infer that the translational ordering of the $\begin{pmatrix}4 & 1\\ 1 & 3\end{pmatrix}$ and the (4×3) phase on the Cu and CuO stripes, respectively, is rather well maintained. No new superstructures with entirely different unit cells appear even on rather narrow stripes. The translational disorder is most apparent for the $\begin{pmatrix}4 & 1\\ 1 & 3\end{pmatrix}$ phase, especially in the vicinity of the lower step edge. More importantly, the orientational ordering of the molecules appears to be quite sensitive to the presence of the step edges. Again, this is most pronounced on the Cu stripes, where the pinwheel ordering is completely suppressed on narrow stripes. The

stronger influence on the $\begin{pmatrix} 4 & 1 \\ 1 & 3 \end{pmatrix}$ pinwheel phase of both the translational and the orientational order can be rationalized as follows: (i) the bottom step edge is the only place where the binding energy is strongly altered. Figure 9 reveals an additional attractive well of about 20 meV and a possible second adsorption site. (ii) The orientation of the high symmetry axis of the $\begin{pmatrix} 4 & 1 \\ 1 & 3 \end{pmatrix}$ phase is not parallel to the [001] direction of the confining step edges. It is conceivable that such a ''symmetry frustration'' might have a strong influence on the long-range ordering.

VI. CONCLUSION

The Cu-CuO surface turns out to be a convenient template to study the influence of step edges and severe lateral confinement on the adsorption and the structure of physisorbed N_2 molecules. The combined experimental and theoretical approach allows a detailed analysis of the adsorption scenario and insights in the driving forces at the atomic scale. We find that the adsorption and growth of a complete monolayer proceeds in three steps: (i) adsorption into a lattice gas phase on top of the CuO stripes, (ii) adsorption on the Cu stripes, and (iii) compression of the lattice gas phase on the CuO stripes. This *selective* adsorption is energetically driven, the energetically most favored sites being occupied first. The $\begin{pmatrix} 4 & 1 \\ 1 & 3 \end{pmatrix}$ and the (4×3) structures of the N_2 adlayer on Cu and CuO, respectively, are influenced by the finite size of the stripe width and, most importantly, by the presence of the step edges. With decreasing stripe width, the phases become increasingly disordered, with the long-range orientational order being particularly sensitive. Yet, the main structural features, such as the adsorption sites and the local configuration at the center of the stripes are preserved. The disorder appears to be more pronounced in the experiment than predicted by theory. Possibly, step-edge defects (kinks) and uncertainties in the potential corrugation at both sides of the step edge could be responsible for the remaining discrepancy. In this context, experiments probing the local energetic and structural properties of the adsorbates and first principles calculations of the adsorption properties in the vicinity of a step edge are needed in the future.

ACKNOWLEDGMENTS

This project was partly supported by the Austrian Fonds zur Förderung der wissenschaflichen Forschung under Contract No. P12317–NAW.

*Electronic address: zeppenfeld@exphys.uni-linz.ac.at
†Present address: Untere Weidenstr. 19, D-81543 München, Germany.

[1] M. Sunderam, S.A. Chalmers, P.F. Hopkins, and A.C. Gossard, Science **254**, 1326 (1991).
[2] V. Marsico, M. Blanc, K. Kuhnke, and K. Kern, Phys. Rev. Lett. **78**, 94 (1997).
[3] D.Y. Petrovykh, F.J. Himpsel, and T. Jung, Surf. Sci. **407**, 189 (1998).
[4] K. Kern, H. Niehus, A. Schatz, P. Zeppenfeld, J. Goerge, and G. Comsa, Phys. Rev. Lett. **67**, 855 (1991); P. Zeppenfeld, M. Krzyzowski, C. Romainczyk, G. Comsa, and M.G. Lagally, *ibid.* **72**, 2737 (1994).
[5] F.M. Leibsle, C.F.J. Flipse, and A.W. Robinson, Phys. Rev. B **47**, 15 865 (1993).
[6] H. Ellmer, V. Repain, S. Rousset, B. Croset, M. Sotto, and P. Zeppenfeld, Surf. Sci. **476**, 95 (2001).
[7] Y. Matsumoto and K. Tanaka, J. Appl. Phys. **37**, L154 (1998).
[8] P. Zeppenfeld, V. Diercks, C. Tölkes, R. David, and M.A. Krzyzowski, Appl. Surf. Sci **130-132**, 484 (1998).
[9] D.J. Coulman, J. Wintterlin, R.J. Behm, and G. Ertl, Phys. Rev. Lett. **64**, 1761 (1990); F. Jensen, F. Besenbacher, E. Laegsgaard, and I. Stensgaard, Phys. Rev. B **41**, 10 233 (1990).
[10] V.I. Marchenko, JETP Lett. **55**, 73 (1992); D. Vanderbilt, Surf. Sci. **268**, L300 (1992).
[11] P. Zeppenfeld, J. Goerge, V. Diercks, R. Halmer, R. David, G. Comsa, A. Marmier, C. Ramseyer, and C. Girardet, Phys. Rev. Lett. **78**, 1504 (1997); A. Marmier, C. Ramseyer, C. Girardet, J. Goerge, P. Zeppenfeld, M. Büchel, R. David, and G. Comsa, Surf. Sci. **383**, 321 (1997).
[12] P. Zeppenfeld, V. Diercks, R. Halmer, R. David, V. Pouthier, C. Ramseyer, and C. Girardet, Surf. Sci. **423**, 175 (1998).
[13] V. Pouthier, C. Ramseyer, C. Girardet, P. Zeppenfeld, V. Diercks, and R. Halmer, Phys. Rev. B **58**, 9998 (1998).
[14] R. David, K. Kern, P. Zeppenfeld, and G. Comsa, Rev. Sci. Instrum. **57**, 2771 (1986).
[15] F. Picaud, C. Ramseyer, C. Girardet, V. Diercks, R. David, and P. Zeppenfeld, Surf. Sci. **482**, 1379 (2001).
[16] For a recent review see D. Marx and H. Wiechert, *Advances Chemical Physics*, edited by I. Prigogine and S.A. Rice (John Wiley, New York, 1996), Vol. 95, p. 213.
[17] L.W. Bruch, M.W. Cole, and E. Zaremba, in *Physical Adsorption: Forces and Phenomena* (Clarendon Press, Oxford, 1997).
[18] R.D. Diehl, M.F. Toney, and S.C. Fain, Jr., Phys. Rev. Lett. **48**, 177 (1982); R.D. Diehl and S.C. Fain, Jr., Surf. Sci. **125**, 116 (1983).
[19] C. Ramseyer, C. Girardet, F. Bartolucci, G. Schmitz, R. Franchy, D. Teillet-Billy, and J.P. Gauyacq, Phys. Rev. B **58**, 4111 (1998); L.W. Bruch and F.Y. Hansen, *ibid.* **57**, 9285 (1998).
[20] P. Zeppenfeld, R. David, C. Ramseyer, P. Hoang, and C. Girardet, Surf. Sci. **444**, 163 (2000).
[21] S. Kirckpatrick, C.D. Gelatt, Jr., and M.P. Vecchi, Science **220**, 671 (1983).